HHS Public Access

Author manuscript

Sci Immunol. Author manuscript; available in PMC 2022 August 14.

Published in final edited form as:

Sci Immunol. 2022 June 10; 7(72): eabh3816. doi:10.1126/sciimmunol.abh3816.

Maternal gut microbiome-induced IgG regulates neonatal gut microbiome and immunity

Katherine Z. Sanidad[1,2,*], **Mohammed Amir**[1,2,*], **Aparna Ananthanarayanan**[1,2], **Anvita Singaraju**[3], **Nicholas B. Shiland**[1], **Hanna S. Hong**[4], **Nobuhiko Kamada**[5,6], **Naohiro Inohara**[4], **Gabriel Núñez**[4], **Melody Y. Zeng**[1,2,3,7,#]

[1]Drukier Institute for Children's Health, Weill Cornell Medicine, New York City, New York

[2]Department of Pediatrics, Weill Cornell Medicine, New York City, New York

[3]Immunology and Microbial Pathogenesis Graduate Program, Weill Cornell Medicine, New York City, New York

[4]Department of Pathology and Rogel Cancer Center, University of Michigan Medical School, Ann Arbor, Michigan

[5]Division of Gastroenterology, Department of Internal Medicine, University of Michigan, Ann Arbor, MI, USA

[6]WPI Immunology Frontier Research Center, Osaka University, Suita, Japan

Abstract

The gut microbiome elicits antigen-specific IgG at steady state that cross-reacts to pathogens to confer protection against systemic infection. The role of gut microbiome-specific IgG antibodies in the development of gut microbiome and immunity against enteric pathogens in early life, however, remains largely undefined. In this study, we show that gut microbiome-induced maternal IgG is transferred to the neonatal intestine through maternal milk via the neonatal Fc receptor and directly inhibits *Citrobacter rodentium* colonization and attachment to the mucosa. Enhanced neonatal immunity against oral *C. rodentium* infection was observed following maternal immunization with a gut microbiome-derived IgG antigen, outer-membrane protein A (OMP-A), or induction of IgG-inducing gut bacteria. Furthermore, by generating a gene-targeted mouse model with complete IgG deficiency, we demonstrate that IgG KO neonates are more susceptible to *C. rodentium* infection, and exhibit alterations of the gut microbiome that promote differentiation of IL-17A-producing γδ T cells in the intestine, which persist into adulthood

[7]Correspondence: M.Y.Z. (myz4001@med.cornell.edu).
[*]Equal contribution
[#]Lead Contact

Author contributions: M.Y.Z. and G.N. conceived this study. M.Y.Z. designed, provided funding, supervised all studies, and wrote the manuscript with feedback from all authors. M.Y.Z., M.A., and K.Z.S. conducted most of the experiments with assistance from A.A., A.S., N.S., and H.H. N.I. provided *E. coli* strains and assistance with bioinformatic analyses. N.K. provided data on adult *Fcgrt*$^{-/-}$ mice.

Competing interests: M.Y.Z. is a consultant for Guidepoint. All other authors declare no competing interests.

Data and materials availability: The 16S sequencing data for this study has been deposited in the BioProject database: PRJNA823289 (Figure 5), PRJNA823357 (Figure 6), PRJNA823359 (Figure S2), and PRJNA823360 (Figure S5). The IgG-deficient mouse strain generated in the course of this study can be requested from M.Y.Z. through a Material Transfer Agreement.

and contribute to increased disease severity in a DSS-induced mouse model of colitis. Taken together, our studies have defined a critical role for maternal gut microbiome-specific IgG antibodies in promoting immunity against enteric pathogens and shaping the development of the gut microbiome and immune cells in early life.

One-sentence summary:

Maternal milk IgG transferred to the neonatal intestine protects against an enteric pathogen and shapes the gut microbiome and immune cells.

INTRODUCTION

Early life is a critical time window for the development of the immune system, which is driven in part by progressive colonization of beneficial bacteria in the maturing neonatal gut (1, 2). Increased susceptibility of infants to enteric pathogens is in part attributable to both immaturity of the immune system and absence of protective bacterial symbionts that inhibit pathogen colonization (3, 4). Neonatal infection is one of the most common causes of neonatal morbidity and mortality, especially in the preterm population. In particular, diarrheal diseases due to enteric infections account for 1 in 9 child deaths worldwide (5). Most of the bacteria responsible for bacteremia are of enteric origin (6, 7). Gram-negative *Escherichia coli (E. coli)* is among the most common bacteria associated with neonatal infections (8).

Maternal antibodies can be transferred placentally prior to birth to the fetus and via breast milk to the neonate after birth (9). After birth, maternal milk provides the first source of antibody-mediated protection in the intestinal tract of infants against infection (10). Increasing evidence has suggested prolonged antibiotic use in infants may lead to dysbiosis of the gut microbiome and increased risks of late-onset sepsis, necrotizing enterocolitis, and mortality (5, 8, 11, 12). The emergence of antibiotic-resistant bacterial strains also presents a challenge to treating neonatal infections (13). Therefore, antibiotic-independent approaches, such as maternal immunization and maternal use of probiotics and prebiotics, are needed to prevent or treat neonatal infections.

Previous studies showed that the gut microbiome can induce antigen-specific IgG that can cross-react with pathogen antigens to promote systemic pathogen eradication in adult mice (14). Additionally, gut microbiome-induced IgG antibodies exhibit biased specificities against gram-negative *Enterobacteriaceae* such as *E. coli* (14), a common causative bacterium in neonatal infections (15). Maternal IgG antibodies were also shown to cooperate with IgA to dampen $CD4^+$ T cells in the neonatal gut (16). The functions of maternal milk IgA antibodies in gut host defense have been well explored (17, 18). The impact of maternal milk IgG on maturation of the gut microbiome in the neonatal gut, however, remains undefined. Recent studies have provided additional evidence to support the potential of maternal immunization as an effective approach to protect neonates from infections (19). A better understanding of the functions of maternal gut microbiome-induced IgG antibodies in the development of intestinal immune cells and gut microbiome during early

life may unravel important regulatory mechanisms underlying immune cell development in the neonatal gut.

In this study, we demonstrate that gut microbiome-induced IgG antibodies are transferred from serum to maternal milk in a process that is facilitated by the neonatal Fc receptor (FcRn), resulting in increased levels of IgG and IgA in the neonatal intestine than in the adult intestine, as well as robust IgG and IgA coating of gut commensal bacteria. Upon enteric infection by *Citrobacter rodentium*, a murine model of enteropathogenic and enterohemorrhagic *E. coli* (EPEC and EHEC, respectively) (20), maternal IgG antibodies in the neonatal gut inhibit attachment of *C. rodentium* to the mucosa. Maternal immunization with a gut microbiome-derived gram-negative IgG antigen, outer-membrane protein A (OMP-A), conferred protection against *C. rodentium* in neonatal mice. Furthermore, using a newly generated mouse model deficient in all IgG isotypes, we show that lacking IgG leads to altered gut microbiome that promotes gut IL-17A-producing γδ T cells at steady state in the IgG KO neonatal intestine and contributes to increased susceptibility to colitis in adulthood.

RESULTS

Maternal IgG antibodies are transferred to maternal milk through FcRn and coat bacteria in the neonatal intestine

We previously reported the presence of gut microbiome-specific IgG antibodies that circulate systemically in adult mice and confer critical protection against systemic infection by pathogens that share conserved IgG surface antigens. These IgG antibodies, however, were scarce in the sera of mice 4 weeks after birth, as well as in the intestinal lumen of adult mice at steady state (14). To appreciate the function of these antibodies in the neonatal gut, we first asked whether neonates acquire these protective IgG antibodies from the mother. We detected robust levels of IgG in WT maternal milk that recognized proteins of gram-negative gut commensal or pathogenic bacteria, *E. coli* and *C. rodentium*, respectively (Figure 1A). During fetal development, maternal antibodies are transported through the placenta to the fetus during the third trimester via the neonatal Fc receptor FcRn (*Fcgrt*) (21). FcRn is expressed at high levels in epithelial cells in human mammary glands to facilitate the transfer of serum IgG to maternal milk (22), as well as in neonatal intestinal enterocytes to facilitate the uptake of maternal milk and transcytosis to circulation (23). We found that the transfer of gut microbiome-specific IgG antibodies to maternal milk is dependent on FcRn as well, as gut microbiome-specific IgG antibodies were almost undetectable in *Fcgrt*$^{-/-}$ maternal milk (Figure 1A).

Binding to FcRn prolongs the half-life of serum IgG. Consistently, we detected a 20–30% reduction in serum IgG1 and IgG2a in adult FcRn-deficient (*Fcgrt*$^{-/-}$) mice (Figure S1A). The amounts of serum IgG against fecal bacteria in adult *Fcgrt*$^{-/-}$ mice were only ~40% of that detected in the sera of WT adult mice (Figure S1B–C). This demonstrates that the scarcity of gut microbiome-specific IgG in *Fcgrt*$^{-/-}$ maternal milk is attributable to two factors: lower levels of serum IgG against gut bacteria in the dam and lacking FcRn to transfer these IgG antibodies from serum to maternal milk.

We further demonstrated that FcRn mediates the transfer of gut microbiome-reactive maternal IgG to the neonatal intestine, which directly targets gut bacteria in neonatal mice (Figure 1B). The same trend was observed for IgA-coating of gut bacteria between neonatal and adult mice (Figure 1C). This may reflect increased abundance of gut microbiome-specific IgG and IgA in the neonatal intestine due to direct supply of maternal milk to the neonatal intestine; whereas in adults, IgG in the intestinal lumen is limited at steady state and increases only in response to gut injury or infection, as implicated in our previous study (14). Furthermore, IgA-coated fecal bacteria from neonates and adults were almost all positive for IgG as well (Figure 1D), suggesting originally within the dam the same population of gut commensal bacteria elicited both IgA and IgG antibody response.

Maternal IgG antibodies opsonize and inhibit colonization and mucosa-attachment of *C. rodentium* in the neonatal gut

Similar clearance of *C. rodentium* was observed in adult *Fcrgt*$^{-/-}$ and WT (*Fcrgt*$^{+/+}$) mice (Figure 2A). To investigate whether maternal IgG antibodies in the neonatal gut confer protection against enteric pathogens in neonates, we orally infected 18-day old WT or *Fcgrt*$^{-/-}$ mice with gram-negative *C. rodentium*. While pathogen loads detected in feces from WT infected neonates gradually increased but started to drop around day 7 following infection, the bacterial loads in *Fcgrt*$^{-/-}$ neonates were detected at higher levels as early as day 2–3 after infection and remained significantly higher beyond day 7 (Figure 2B). This suggests a possible inhibitory effect of maternal IgG on the colonization of *C. rodentium* in the neonatal gut. In contrast to almost complete protection against infection in WT and IgA-deficient neonates, we observed 100% mortality in *Fcgrt*$^{-/-}$ neonates, akin to that found in B cell-deficient $J_H^{-/-}$ mice (Figure 2C). Of note, stool bacteria of *Fcgrt*$^{-/-}$ neonates transplanted into germ-free (GF) neonates showed similar colonization resistance against *C. rodentium* as stool bacteria from WT neonates (Figure 2D), indicating the increased mortality in *Fcgrt*$^{-/-}$ neonates (Figure 2C) was likely due to lack of maternal IgG rather than reduced colonization resistance against *C. rodentium* by the gut bacteria in *Fcgrt*$^{-/-}$ neonates. To understand the mechanisms underlying maternal IgG-mediated protection, we orally infected WT, B cell-deficient $J_H^{-/-}$ (24), or *Fcgrt*$^{-/-}$ neonates with a GFP-expressing strain of *C. rodentium*. On day 6 post infection, ~10% luminal GFP-*C. rodentium* with surface IgG coating was observed in WT infected mice, in contrast to almost complete absence of IgG-coated luminal GFP-*C. rodentium* in *Fcgrt*$^{-/-}$ mice (Figure 2E). Previous studies showed that virulent *C. rodentium* is able to adhere to the intestinal mucosa, and inability to inhibit attachment of virulent *C. rodentium* to the intestinal mucosa is associated with increased penetration through the intestinal epithelium and systemic dissemination of *C. rodentium* (25). To assess whether IgG-coating would affect the adherence of virulent *C. rodentium* to the mucosa, we used a strain of *C. rodentium* that expressed luminescence under the Ler promoter (*C. rodentium-ler-lux*), which allowed detection of *C. rodentium* expressing Ler-dependent virulence factors in vivo (26). After removing luminal contents prior to imaging, we found increased luminescence-expressing mucosa-associated *C. rodentium* on the ceca and colons of infected *Fcgrt*$^{-/-}$ neonates compared to WT neonates 6 days after infection, which persisted even on day 12 following infection (Figure 2F). In addition, the colon length of infected *Fcgrt*$^{-/-}$ neonates was noticeably shorter than that of WT mice, thus consistently indicating increased intestinal inflammation in infected

Fcgrt$^{-/-}$ neonates (Figure 2F). These observations indicated increased adherence of virulent *C. rodentium* to the mucosa in the absence of IgG. Consistently, increased numbers of translocated *C. rodentium* were detected in the blood, spleens and livers of *Fcgrt*$^{-/-}$ neonates (Figure 2G), likely leading to the ultimate demise of these mice (Figure 2C).

Since maternal IgG antibodies are transferred placentally during pregnancy and via maternal milk after birth, to delineate the contributions of prenatal and postnatal transfer of maternal IgG antibodies to neonatal immune defense against enteric infection, WT newborns were cross-fostered with a *Fcgrt*$^{-/-}$ dam immediately after birth. Upon oral infection with *C. rodentium*, the fostered neonates exhibited increased mortality (>70%) compared to 100% survival in littermates that were nursed by biological WT dams (Figure 2H). This result suggests postnatal maternal IgG transfer through maternal milk accounts for most of the immune protection by maternal IgG against enteric gram-negative pathogens in neonates.

Colonization of IgG-inducing gut bacteria, or maternal immunization with OMP-A, confers protection against enteric infection via induction of IgG

To further elucidate the role of the gut microbiome in the induction of protective IgG against *C. rodentium*, we isolated luminal bacteria with or without IgG coating from 3-week-old WT mice, which were inoculated by oral gavage into 3-week-old WT germ-free (GF) mice (Figure S2A–C). Two weeks later, serum IgG antibodies against fecal bacteria were induced at higher levels in the ex-GF mice that were transplanted with IgG-coated bacteria (IgG^{+} exGF) compared to that in mice transplanted with bacteria not coated with IgG (IgG- exGF) (Figure 3A). Of note, there was no difference in the amount of serum IgA against fecal bacteria between the two groups of mice. Despite differential abundance of some bacterial taxa in IgG^{+} exGF mice, there was no apparent gut inflammation in either group prior to *C. rodentium* infection (Figure S2B–C). Importantly, following oral infection with *C. rodentium*, we detected lower numbers of translocated *C. rodentium* in the spleens and livers of IgG^{+} exGF mice (Figure 3B). Taken together, our results further demonstrated protection against *C. rodentium* by IgG-inducing gut bacteria.

Furthermore, to test whether maternal immunization to increase gut microbiome-specific IgG would enhance neonatal immunity, potential gut microbiome-derived IgG antigens from the outer membrane of *E. coli* K12 was immunoprecipitated using purified IgG from naïve WT adult mouse sera (Figure S2D). Immunoprecipitated proteins were analyzed by mass spectrometry. One of the top proteins identified was outer membrane protein (OMP) (Figure S2E), which is present in all gram-negative *Enterobacteriaceae* (27). To verify the presence of anti-OMP IgG in mice, we used cell lysates from *E. coli* strains that were deficient in one of the known OMPs (OMPs C, A, F and X), and confirmed the presence of anti-OMP-A IgG in sera from naïve adult WT mice (Figure 3C). Furthermore, we immunized female mice with purified OMP-A prior to mating and re-boosted with OMP-A administration two weeks later, which resulted in increased levels of anti-OMP-A serum IgG in immunized females (Figure S2F). The offspring from the immunized or non-immunized dams were orally infected with a high dose of *C. rodentium* (5×10^{8}), which caused 100% mortality in the offspring from non-immunized dams, in contrast to ~20% mortality and lower bacterial loads in the blood in the offspring from immunized dams (Figure 3D–E). Importantly,

the protection conferred by maternal immunization was absent in *Fcgrt*$^{-/-}$ mice (Figure 3F) and independent of IgA (Figure 3G), thus suggesting the protection was mediated through induction of IgG antibodies. Collectively, our data suggested the importance of gut microbiome as a source of IgG antigens to elicit homeostatic IgG that can be transferred via maternal milk to confer critical protection against enteric pathogens in neonates.

IgG-deficient neonatal mice are more susceptible to enteric *C. rodentium* infection

To further investigate how lacking maternal IgG may affect gut immune response and susceptibility to enteric infection in neonatal mice, we generated a mouse model that is deficient in all IgG isotypes (IgG1, 2a, 2b and 3) by deleting >80 kb of DNA fragments containing the mouse IgG-encoding loci using a CRISPR-Cas 9 gene editing system (Figure S3A–C). The founders were on B6 background and were further backcrossed to the B6 background for more than 10 generations. Deficiency of all IgG isotypes was confirmed in the IgG KO mice, while serum IgA, IgE, and IgM were intact in these mice compared to WT littermates (Figure 4A and S3C). Consistent with findings in *Fcgrt*$^{-/-}$ neonates, P7 and P14 IgG KO neonates showed increased systemic translocation of *C. rodentium* (Figure 4B–C), increased gut barrier permeability and intestinal inflammation (Figure S3D–E) and mortality following *C. rodentium* infection (Figure 4D).

IgG deficiency in neonates is associated with alterations in the gut microbiome and increased IL-17A-producing cells in the intestine

To investigate whether lacking maternal IgG would affect the composition of gut microbiome, we analyzed the gut microbiome in IgG KO and WT littermates that were separated right after birth and nursed by IgG KO and heterozygous foster dams (both dams were littermates that were co-housed until used for cross-fostering), respectively. We found differential abundance of several Operational Taxonomic Units (OTUs) within the bacterial populations in both the small intestines and colons of 2-weeks-old IgG KO and WT neonates (Figure 5A). Specifically, in the colon, two OTUs of *Porphyromonadaceae* in particular were more abundant in WT than IgG KO neonates. Additionally, while an OTU of gram-positive *Lactobacillus* was more abundant in WT SI, an OTU of gram-negative *Enterobacteriaceae* and an OTU of *Prevotellaceae* were more abundant in IgG KO SI (Figure 5A).

Additionally, to determine whether IgG deficiency may change gut immune cell responses in the neonatal gut, we analyzed lamina propria cells in 2-week-old IgG KO and WT neonates. We found increased numbers of IL-17A-producing cells within the $CD3^{+}CD4^{-}CD45^{+}$ lymphocyte populations in both the small intestines and colons of IgG KO neonates (Figure 5B–C, S4A–B). Consistent with the enhanced IL-17A response, we found increased neutrophils in the colons of IgG KO neonatal colons (Figure 5D, S4C). Of note, almost all of these IL-17A-producing cells expressed a γδ TCR, suggesting they were γδ T cells (Figure 5E). In addition, these IL-17A-producing γδ T cells were diminished in WT germ-free (GF) neonates compared to specific-pathogen-free (SPF) WT neonates (Figure S4D), suggesting the gut microbiome as a driver of the development of γδ T cells in the neonatal gut. To determine whether increased IL-17A production in the IgG KO neonatal gut was driven by altered gut microbiome in these mice, we re-derived IgG KO mice germ-free (Figure 5F). Similar numbers of IL-17A-producing $CD3^{+}$ T cells were observed in WT and IgG KO GF

mice (Figure 5G). Additionally, 2 weeks following oral transplantation of stool from P7 SPF WT or IgG KO stool into P7 WT GF neonates, we found increased IL-17A$^+$ γδ T cells and IL-17A$^+$ CD4$^+$ cells in the intestines of the recipient mice with stool from IgG KO donors (Figure 5H, S4E). Furthermore, cross-fostering by a WT dam immediately after birth led to reduced numbers of IL-17A$^+$ γδ T cells and IL-17A$^+$ CD4$^+$ cells in IgG KO P14 neonates (Figure 5I, S4F). Collectively, our findings suggest that postnatal maternal IgG is critical to dampen intestinal IL17-producing γδ T cells in neonates via regulation of the gut microbiome.

Altered gut microbiome increases the susceptibility to DSS-induced colitis in IgG KO adult mice

To investigate whether the role of gut microbiome-specific IgG in shaping gut microbiome and immune cells is restricted to the early developmental stage, IgG KO and WT adult mice (at least 8 weeks of age) were first co-housed for two weeks before separation and induction of colitis by administration of 2% dextran sulfate sodium (DSS) in drinking water for 7 days. Reduction in colon lengths, an indicator of disease severity, was more pronounced in DSS-treated IgG KO mice (Figure 6A), with increased numbers of IL-17A-producing colonic lamina propria T cells and macrophages (Figures 6B, S5A). Despite homogenization of the gut microbiome between IgG KO and WT mice after two weeks of co-housing, the gut microbiome appeared to diverge during the course of DSS treatment during which these mice were separated (Figures 6C–E). For example, an OTU corresponding to *Akkermansia* was significantly reduced in IgG KO DSS-treated mice, which had enriched *Erysipelotrichaceae* (Figure 6D). This suggests IgG antibodies are important to control the gut microbiome in adults as well, which might be even more critical in the setting of gut inflammation where opportunistic gut bacteria over-bloom and further exacerbate gut injury. To further interrogate the role of the gut microbiome in the altered immune response to DSS in IgG KO mice, IgG KO and WT adult mice were first co-housed for two weeks before DSS treatment and remained co-housed throughout the DSS treatment (Figures 6F–G). The differences in the composition of the gut microbiome, colon shortening and colonic lamina propria immune cells, including IL-17A$^+$ T cells, were no longer observed between the two genotypes (Figures 6F–G, S5B–E), thus suggesting the gut microbiome was a driver in the increased gut inflammation in IgG KO DSS-treated mice when housed separately from WT mice (Figures 6A–E). Of note, in naïve WT mice, we found that co-housing with IgG KO mice led to increased numbers of IgG-coated fecal bacteria, implicating the transfer of IgG-targeting bacteria that over-bloom in IgG KO mice to the WT co-housed mice. Consistently WT mice co-housed with IgG KO mice during the course of DSS treatment had increased IL-17A$^+$ intestinal cells to the levels observed in the co-housed IgG KO mice (Figure 6G); this suggests the transferred IgG-coated bacteria (Figure S5F) in the WT co-housed mice were likely a driver of the IL-17A response. Together, these findings demonstrate that the critical role for IgG to control the gut microbiome and immune cells extends beyond the early developmental period.

DISCUSSION

Our studies have demonstrated that gut microbiome-specific maternal IgG antibodies are transferred to the neonatal intestine through breast milk via FcRn, resulting in increased levels of these IgG antibodies in the neonatal intestine than in the adult intestine. These antibodies directly cross-react with the enteric pathogen *C. rodentium* to suppress colonization and attachment to the mucosal epithelium to confer critical protection in neonates. Furthermore, we showed that colonization of germ-free mice with IgG-inducing gut commensal bacteria, or maternal immunization with a gut bacteria-derived IgG antigen, led to protection against *C. rodentium* enteric infection in an IgG-dependent manner. Additionally, we generated a gene-targeted mouse model deficient in all IgG isotypes. Alterations of the gut microbiome in IgG KO neonates promote IL-17A-producing T cells in IgG KO neonatal intestines. The integral role for IgG to control gut bacteria and regulate intestinal immune cells extends into adulthood and represents an important mechanism to maintain gut homeostasis.

The function of IgG antibodies is conventionally linked primarily to systemic infection. In systemic infection, antigen-specific IgG antibodies opsonize pathogens and facilitate phagocytosis of pathogens via binding to Fc receptors on phagocytes. Such an effector function, however, might not be the primary function of luminal IgG to confer protection in the neonatal lumen, as phagocytes are almost absent in the gut lumen at steady state or in the initial phase of enteric infection. Our studies showed that maternal IgG antibodies in the neonatal gut directly bound to *C. rodentium* and diminished gut colonization and attachment of virulent *C. rodentium* to the mucosa. A previous study reported differential localization of *C. rodentium* in the gut, with avirulent *C. rodentium* mainly localized in the lumen of the gut while virulent *C. rodentium* was capable of attaching to the mucosa (14, 28). The mucosa of the neonatal gut (epithelium and the mucus layer) is not fully developed and more vulnerable to bacterial translocation upon attachment of pathogens. We have demonstrated the presence of IgG antibodies in breast milk that cross-react to enteric pathogens via IgG antigens conserved in gut commensals. The increased availability of IgG in the neonatal gut through breast milk may create a unique phenomenon in which IgG is readily accessible to gut bacteria to confer protection against pathobionts or enteric pathogens without requiring damage of the gut epithelium for IgG access to the gut lumen as seen in enteric infection in adults. We previously showed that at steady state in adult mice, there is almost complete absence of gut microbiome-specific IgG antibodies in the gut lumen (14). Our findings in the current study thus shed light on an unconventional and localized function of IgG in the neonatal gut, with the capability for direct binding to inhibit gut colonization and attachment of enteric pathogens to the gut mucosa during the initial stage of enteric infection.

Our characterization of the IgG KO neonatal gut revealed a selective increase in the abundance of gram-negative *Enterobacteriaceae* and *Prevotellaceae* in the small intestine in the absence of maternal IgG. This is consistent with our previous finding of a bias towards gram-negative *Enterobacteriaceae* in IgG antibodies that are induced by the gut microbiome at steady state (14). *Enterobacteriaceae* is one of the earliest bacterial colonizers in the neonatal gut in which the relative higher oxygen content can be tolerated by these bacteria (29, 30). However, expansion of *Enterobacteriaceae* is known to induce more

gut inflammation in inflammatory bowel disease (IBD) or necrotizing enterocolitis (NEC) (31–33). Our data suggest acquisition of IgG antibodies through maternal milk might be an important mechanism to inhibit the expansion of *Enterobacteriaceae* in the developing neonatal gut, which might be necessary and critical to allow establishment of subsequent bacterial colonizers in the neonatal gut, such as beneficial *Clostridiales* and *Bacteroidales* species for normal development of the gut microbiome (3, 12). Additionally, our results show a propensity to develop IL-17A-producing γδ T cells in the IgG KO neonatal gut, which is driven by alterations of the gut microbiome. Overgrowth of *Enterobacteriaceae* is associated with induction of IL-17 and gut inflammation in mouse models of colitis (31, 34). Previous studies showed that transient gestational maternal bacterial colonization impacts immune cell development in the neonatal gut (2), and maternal IgG and IgA cooperate to dampen mucosal $CD4^+$ T cells in neonates (16). In line with these reports, our finding of an IL-17A-biased immune cell response in IgG KO neonatal gut demonstrates another function of maternal IgG in the regulation of intestinal immune cells in early life. IL-17 is a common driver of inflammation in autoimmune diseases, such as IBD and multiple sclerosis (35). Importantly, our data demonstrate that the role of the IgG-gut microbiome interplay in dampening IL-17A responses in the intestine extends into adulthood to orchestrate gut inflammation via regulation of the gut microbiome.

Our data also suggest colonization of the neonatal gut with IgG-coated bacteria confers protection against enteric pathogens in the neonates by inducing protective IgG. We show that the IgA-coated bacteria in the neonatal gut were coated by IgG as well. Interestingly, previous studies showed that transplantation of IgA-coated bacteria into germ-free mice led to more exaggerated gut inflammation in mouse models of colitis or NEC (36) (37). This may be consistent with our hypothesis that IgG-coated bacteria (which are the same as IgA-coated bacteria) in the neonatal intestine represent the bacteria that would otherwise expand in the absence of IgG (and possibly IgA) and cause gut inflammation. There are notable differences in the function of IgG and IgA in general. IgG antibodies are known to play a more profound role in systemic infections and exhibit enhanced specificities and affinity for pathogens; while the functions of IgA are more restricted to the mucosal surface to promote beneficial interactions with the microbiome (38). There might be nonredundant immune signaling pathways mediated by IgG-FcγR and IgA-FcαRI cross-linking in myeloid cells as well. Further investigation is needed to delineate whether there are nonredundant roles for maternal milk IgG and IgA in both the regulation of the gut microbiome and immune responses in early life.

Of note, a recent study demonstrated the requirement for FcRn in mediating the transfer of maternal IgG to the circulation in neonates, which is important to protect neonates from systemic infection (39). Therefore, IgG from maternal milk may circulate from the neonatal gut into circulation to confer protection beyond the gut. The present study is focused on interrogating the role of maternal IgG in immunity and immune development in the neonatal intestine. Our findings demonstrate that maternal gut microbiome-specific IgG antibodies shape the development of the gut microbiome and dampen $IL\text{-}17A^+$ cells, and enhance host defense against enteric infections in early life. This critical function of the gut microbiome-specific IgG might be leveraged in developing preventive or therapeutic strategies, such as maternal immunization or colonization with beneficial bacteria of interest,

to strengthen neonatal immunity against enteric pathogens and facilitate proper development of the gut microbiome and immune cells in infants.

MATERIALS AND METHODS

Study Design

The aim of this study was to investigate the role of maternal gut microbiome-reactive IgG antibodies in the regulation of neonatal immunity against enteric bacterial pathogens, and the development of the gut microbiome and immune cells in the neonatal offspring. We employed flow cytometry to identify IgG-coated gut commensal and pathogenic bacteria, a mouse model of enteric infection with *C. rodentium*, gnotobiotic mice to induce gut microbiota-specific IgG, and lastly, a genetic model of complete IgG deficiency to analyze the development of neonatal gut microbiome and immune cells in the absence of IgG.

Mice

Wild-type and *Fcgrt*$^{-/-}$ mice (B6.129X1-*Fcgrt*^{tm1Dcr}/DcrJ; strain 003982) on a C57BL/6 background were originally purchased from the Jackson Laboratory. IgA-deficient mice were originally from Dr. Bernard Arulanandam (40). $J_H^{-/-}$ mice were kindly provided by Marilia Cascalho (Univ. of Michigan) (41). All animal experiments were approved by the Institutional Animal Care and Use Committee at Weill Cornell Medicine.

Isolation of mouse intestinal lamina propria cells

Mouse intestines were removed, cleaned from remaining fat tissue, and washed in ice-cold phosphate-buffered saline (PBS) (Corning). Intestines were opened longitudinally, washed in ice-cold PBS, and cut into small pieces (~2mm). Dissociation of epithelial cells was performed by incubation on a shaker in Hanks' balanced salt solution (Sigma-Aldrich) containing 5 mM EDTA (Thermo Fisher Scientific), 1 mM dithiothreitol (DTT) (Sigma-Aldrich), and 2% heat-inactivated fetal bovine serum (FBS) for 15 min each at 37°C in a glass beaker with stirring. The dissociated cells were filtered through a 70um cell strainer and washed one time prior to enzymatic digestion in digestion buffer containing dispase (0.4 U/ml; Thermo Fisher Scientific), collagenase III (1 mg/ml; Worthington), and deoxyribonuclease (DNase) I (20 μg/ml; Sigma-Aldrich) in 10% FBS/Dulbecco's modified Eagle's medium (DMEM) (Corning) for 30 min at 37°C. Leukocytes were further enriched by a 40/75% Percoll gradient centrifugation (GE Healthcare) at 700g for 20 min.

***C. rodentium* oral infection—**The kanamycin-resistant (Kan^R) WT *C. rodentium* strain DBS120 (pCRP1::Tn5) was a gift of Dr. David *Schauer* (Massachusetts Institute of Technology). The isogenic *C. rodentium ler*-lux reporter strain (Kan^R), and GFP-expressing *C. rodentium* strain (Chloramphenicol resistant; Chl^R) have been described previously (25). For in vivo infection, bacteria were grown overnight in Luria-Bertani (LB) broth supplemented with Kan (50 μg/ml) with shaking at 37°C. Mice were infected by oral gavage with 0.2 ml of PBS containing approximately 0.5–5 × 10^8 CFU of *C. rodentium*. To determine bacterial numbers in the feces, fecal pellets were collected from individual mice, homogenized in cold PBS, serially diluted and plated onto MacConkey agar plates containing 50 μg/ml Kan, and the number of CFU was determined after overnight incubation

at 37°C. Translocated in the spleens and livers of infected mice were enumerated similarly after plating homogenized and diluted tissues in PBS.

Milk collection from mice

Milk collection from mice was performed as previously described (19). Briefly, nursing dams (P7-P16) were separated from their pups for 4–6 h to allow accumulation of milk, followed by anesthetization using 2% isoflurane (VetOne), and 2–8 units per mouse of oxytocin (Sigma) was administered intraperitoneally to induce milk flow. Samples were collected using an electric human breast pump that was modified to accommodate mice and small liquid volumes. All milk was stored at −20°C until use. For western blotting, mouse milk was diluted 1:100. For ELISA, mouse milk was diluted 1:10.

Measurement of Mucosa-Associated C. rodentium

For detection of mucosa-attached *C. rodentium*, WT or *Fcgrt*$^{-/-}$ neonatal mice were infected with ~0.5×10^8 CFU of a LER-driven bioluminescence-expressing strain of *C. rodentium (C. rodentium* ler-lux). Both the cecal and colonic tissues were harvested 6 or 12 days after infection. To remove non-adherent *C. rodentium*, luminal contents in the cecum and colon were flushed with PBS and further washed by with sterile PBS twice. Washed tissues were immediately placed into the light-tight chamber of a CCD *in vivo* imaging system (IVIS 200, PerkinElmer) and bioluminescence in the tissue was captured using the software Living Image (PerkinElmer), as previously described (25). Both control and treatment groups were analyzed at the same time and using the same software settings.

ELISA for bacteria-specific antibodies

For measurement of commensal bacteria or *C. rodentium*-specific IgG, IgM, and IgA, fecal bacteria were isolated from naive WT SPF mice (8–10 weeks old) used to coat ELISA plates as described in our previous studies. Fecal bacteria from ~200 mg fecal pellets were isolated by homogenization in sterile PBS, filtered through a 40 μm cell strainer, and separated from debris/mouse cells by removing the pellet after centrifugation at 1,000 rpm for 5 min. Isolated fecal bacteria were washed twice, heat-killed at 85°C for 1 hr, and resuspended in 10 ml coating buffer, and100 μL was added to each well of a 96-well ELISA plate for overnight coating at 4°C. Mouse sera were diluted at 1:20 and 1:100 and incubated overnight at 4°C for detection of IgG, IgM, and IgA. Anti-mouse IgG and HRP substrate were purchased from Bethyl Laboratories. Anti-mouse IgA and IgM were from Southern Biotech.

Flow cytometry analysis of bacteria—Two mouse fecal pellets were soaked in 1 ml of PBS for 10 min and homogenized (~100 μg/mL). Large debris were removed by centrifuging at 1000 rpm for 30 seconds; the supernatant containing bacteria was transferred to a new 1.5 ml microcentrifuge tube. Bacteria were pelleted at 6000 rpm for 5 min and resuspended in PBS and passed through a 70 μm cell strainer. The bacteria were blocked with 10% FBS for 15 min on ice, washed with FACS buffer (PBS + 1% BSA), and stained with a cocktail of SYTO BC dye (1:4000 dilution, ThermoFisher Scientific S34855), PE-conjugated rat anti-mouse IgA (1:100 dilution, eBioscience clone mA-6E1) and APC-conjugated goat anti-mouse IgG (1:100 dilution, Invitrogen) for 20 min on ice. After that

each sample was washed twice with FACS buffer and acquired on a flow cytometer (Cytek Aurora).

To analyze IgG-coated GFP-*C. rodentium*, colonic or cecal bacteria from infected mice were homogenized in cold sterile PBS (100 μg/mL) thoroughly as described above, filtered through a 70 μm cell strainer, and centrifuged at 900 × *g* for 5 min to remove debris and mouse cells in the pellet. Luminal bacteria in the supernatant were washed several times with cold PBS, pelleted by centrifugation at 3,700 × *g* for 10 min, and stained with APC-anti mouse IgG.

Flow cytometry on lamina propria cells

Lamina propria cells from mouse intestines were isolated as previously described, followed by stimulation for 4 hours ex vivo with phorbol 12-myristate 13-acetate (PMA; 100 ng/ml; Sigma-Aldrich) and ionomycin (1 μg/ml; Sigma-Aldrich) in the presence of brefeldin A for the last hours (10 μg/ml; Sigma-Aldrich) in a 37°C incubator (5% CO_2). Cells were washed with cold PBS and surface-stained before fixation and permeabilization using the Cytofix/Cytoperm Fixation/Permeabilization solution and Perm/Wash buffer according to the manufacturer's protocol (BD Biosciences). Stained bacteria/mouse lamina propria cells were then washed with FACS buffer once, and analyzed by BD Aurora (BD Bioscience). Data were analyzed by Flow Jo (Tree Star).

Maternal immunization and infection

50 μg of recombinant outer membrane protein A (OMP-A; Creative BioMart) was mixed 1:1 (v/v) with Imject Alum (Thermo Fisher Scientific) and IP injected into female mice (WT, *Fcgrt*$^{-/-}$, IgG-deficient, and IgA-deficient) 2 days prior to mating. A second protein/alum injection was administered 2 weeks later (approximately one week prior to giving birth). Pups from naïve or immunized females were orally infected with 5 × 10^8 *C. rodentium* and the survival of the pups was monitored. Some infected pups were euthanized at 6 days following infection to enumerate translocated *C. rodentium* in the spleens and livers.

Generation of IgG-deficient mice

IgG-deficient mice were generated using the CRISPR/Cas9 system. Cas9 mRNA and sgRNA were designed as described previously (42). Briefly, *Cas9* mRNA and sgRNAs were microinjected into fertilized embryos of C57BL/6J mice to allow Cas9-mediated cleavage of DNA sequences about ~1kb upstream of *Ighg3* and ~1kb downstream of *Ighg2b* (performed by the University of Michigan Transgenic Animal Model Core). Deletion of a ~80kb DNA fragment containing all IgG-encoding loci (*Ighg1, Ighg2*a, Ighg*2b and Ighg3*) was confirmed by Sanger sequencing of PCR amplicons (935 bp) of potential founders using genotyping primers The genotyping primers and the full predicted amplicon sequence are provided in the Supplementary Methods. The embryos were transferred into pseudopregnant C57BL/6 females. Confirmed founders from the offspring were additionally mated with C57BL/6 WT mice and subsequent crossing of heterozygous offspring for >10 generations. ELISA for serum IgG was performed to confirm loss of all IgG isotypes in IgG-deficient mice.

16S rRNA gene sequencing—Bacterial genomic DNA was extracted from fecal pellets using the E.Z.N.A. stool DNA kit (Omega Bio-tek) and DNA amplicons of the V4 region within the 16S rRNA gene and sequenced the fragments using an Illumina MiSeq instrument. The sequences were curated using mothur (v.1.35) and sequences were binned into OTUs at >97 % sequence level. LEfSe Linear discriminant analysis (LDA) was performed by the Mothur command using all OTU reads. The OTUs shown in the LEfSe panels are those whose abundance was statistically different with $p < 0.05$.

Fecal transplantation of WT and IgG KO bacteria into GF neonates

P7 WT or IgG KO mice were sacrificed and the luminal contents from the small intestine and colon were collected and homogenized in PBS (~10 μL/mg of luminal contents). P7 GF WT were given the 50 μL of the homogenate by oral gavage. After 2 weeks, the mice were sacrificed and the colons were collected for further analysis of lamina propria immune cells.

Cross-fostering of IgG KO neonates with WT dams

Postnatal day 1 (P1) IgG KO mice were given to either a nursing IgG KO dam or nursing WT dam (see schematic). After 2 weeks, P14 mice were sacrificed and their colons were collected for further analysis of lamina propria immune cells.

***C. rodentium* oral infection in P7 WT and IgG KO mice—**For in vivo infection, Chloramphenicol-resistant (Chl^R) *C. rodentium* (25) was grown overnight in Luria-Bertani (LB) broth supplemented with Chl (10 μg/ml) with shaking at 37°C. P7 WT or IgG KO mice were infected by oral gavage with 50 μL of PBS containing approximately 5×10^5 CFU of *C. rodentium* 3 days post infection, mice were sacrificed and tissues were collected. To determine bacterial numbers in the colon, colon luminal contents were collected from individual mice, homogenized in cold PBS, serially diluted and plated onto MacConkey agar plates containing 25 μg/ml Chl, and the number of CFU was determined after overnight incubation at 37°C. Translocated bacteria were enumerated similarly after plating homogenized and diluted tissues in PBS.

***C. rodentium* oral infection into GF mice with *Fcgrt*$^{-/-}$ or WT mouse fecal transplant—**Fecal pellets from P14 WT or *Fcgrt*$^{-/-}$ mice were collected and homogenized in PBS (200 μL/pellet). P14 GF WT mice were given 50 μL of homogenate via oral gavage. After 4 days, mice were infected with by oral gavage with 5×10^7 CFU of Chl^R *C. rodentium*. *Three days post infection,* mice were sacrificed and tissues were collected. To determine bacterial numbers in the colon, colon luminal contents were collected from individual mice, homogenized in cold PBS, serially diluted and plated onto MacConkey agar plates containing 25 μg/ml Chl, and the number of CFU was determined after overnight incubation at 37°C. Translocated bacteria were enumerated similarly after plating homogenized and diluted tissues in PBS.

FITC-dextran permeability after C. rodentium infection

For in vivo infection, Chloramphenicol-resistant (Chl^R) *C. rodentium* was grown overnight in Luria-Bertani (LB) broth supplemented with Chl (10 μg/ml) with shaking at 37°C. P14 WT or IgG KO mice were infected by oral gavage with 100 μL of PBS containing 5×10^7

CFU of *C. rodentium.* Three days post infection, the mice were fasted for 4 hours. Mice were then given FITC-dextran (500 mg/kg body weight dissolved in PBS, Sigma Aldrich) via oral gavage. After 1 hour, blood was collected and fluorescence intensity in the serum was determined using a spectrophotometer (excitation 485 nm; emission 525 nm).

Statistical analyses—Statistical analyses were performed using GraphPad Prism 7.0 (GraphPad Software). Differences between two groups were evaluated using Student's unpaired t-test (parametric) or Mann-Whitney U test (non-parametric). For multiple comparisons, one-way ANOVA (parametric) with Tukey's multiple comparisons test or Kruskal-Wallis test (non-parametric) were used. Differences with p-values < 0.05 were considered significant.

Supplementary Material

Refer to Web version on PubMed Central for supplementary material.

Acknowledgments:

We thank Thom Saunders (University of Michigan Transgenic Animal Model Core) for assistance with the generation of IgG KO mice, Thomas Miller (Weill Cornell Medicine) for flow cytometry, Rielmer Pinedo from the Gnotobiotic Animal Facilities (WCM) for husbandry of germ-free mice and assistance with re-derivation of IgG KO mice, and the Gut Microbiome Research Core at WCM for their support.

Funding:

This work was supported by NIH grant 5 K01 DK114376, funds from the Gale and Ira Drukier Institute for Children's Health and Children's Health Council at Weill Cornell Medicine, grants from the Center for Immunology, Office of Academic Integration of Cornell University, Center for IBD Research at Weill Cornell Medicine, and the Hartwell Foundation (all to M.Y.Z.), NIH grant R01 DK095782 (to G.N.), and a postdoctoral fellowship from the Hartwell Foundation (to K.Z.S.).

REFERENCES AND NOTES

1. Yatsunenko T et al. , Human gut microbiome viewed across age and geography. Nature 486, 222–227 (2012). [PubMed: 22699611]
2. Gomez de Aguero M et al. , The maternal microbiota drives early postnatal innate immune development. Science 351, 1296–1302 (2016). [PubMed: 26989247]
3. Kim YG et al. , Neonatal acquisition of Clostridia species protects against colonization by bacterial pathogens. Science 356, 315–319 (2017). [PubMed: 28428425]
4. Chernikova DA et al. , The premature infant gut microbiome during the first 6 weeks of life differs based on gestational maturity at birth. Pediatr Res 84, 71–79 (2018). [PubMed: 29795209]
5. Liu L et al., in Reproductive, Maternal, Newborn, and Child Health: Disease Control Priorities, Third Edition (Volume 2), Black RE, Laxminarayan R, Temmerman M, Walker N, Eds. (Washington (DC), 2016).
6. MacFie J, Current status of bacterial translocation as a cause of surgical sepsis. British medical bulletin 71, 1–11 (2004). [PubMed: 15596865]
7. Sedman PC et al. , The prevalence of gut translocation in humans. Gastroenterology 107, 643–649 (1994). [PubMed: 8076751]
8. Polin RA, Committee on F, Newborn, Management of neonates with suspected or proven early-onset bacterial sepsis. Pediatrics 129, 1006–1015 (2012). [PubMed: 22547779]
9. Harris NL et al. , Mechanisms of neonatal mucosal antibody protection. J Immunol 177, 6256–6262 (2006). [PubMed: 17056555]

10. Mantis NJ, Rol N, Corthesy B, Secretory IgA's complex roles in immunity and mucosal homeostasis in the gut. Mucosal immunology 4, 603–611 (2011). [PubMed: 21975936]
11. Singer JR et al. , Preventing dysbiosis of the neonatal mouse intestinal microbiome protects against late-onset sepsis. Nat Med 25, 1772–1782 (2019). [PubMed: 31700190]
12. Yassour M et al. , Natural history of the infant gut microbiome and impact of antibiotic treatment on bacterial strain diversity and stability. Sci Transl Med 8, 343ra381 (2016).
13. Mohsen L et al. , Emerging antimicrobial resistance in early and late-onset neonatal sepsis. Antimicrob Resist Infect Control 6, 63 (2017). [PubMed: 28630687]
14. Zeng MY et al. , Gut Microbiota-Induced Immunoglobulin G Controls Systemic Infection by Symbiotic Bacteria and Pathogens. Immunity 44, 647–658 (2016). [PubMed: 26944199]
15. Bergin SP et al. , Neonatal Escherichia coli Bloodstream Infections: Clinical Outcomes and Impact of Initial Antibiotic Therapy. Pediatr Infect Dis J 34, 933–936 (2015). [PubMed: 26065862]
16. Koch MA et al. , Maternal IgG and IgA Antibodies Dampen Mucosal T Helper Cell Responses in Early Life. Cell 165, 827–841 (2016). [PubMed: 27153495]
17. Rogier EW et al. , Secretory antibodies in breast milk promote long-term intestinal homeostasis by regulating the gut microbiota and host gene expression. Proc Natl Acad Sci U S A 111, 3074–3079 (2014). [PubMed: 24569806]
18. Macpherson AJ, Geuking MB, Slack E, Hapfelmeier S, McCoy KD, The habitat, double life, citizenship, and forgetfulness of IgA. Immunol Rev 245, 132–146 (2012). [PubMed: 22168417]
19. Caballero-Flores G et al. , Maternal Immunization Confers Protection to the Offspring against an Attaching and Effacing Pathogen through Delivery of IgG in Breast Milk. Cell Host Microbe 25, 313–323 e314 (2019). [PubMed: 30686564]
20. Crepin VF, Collins JW, Habibzay M, Frankel G, Citrobacter rodentium mouse model of bacterial infection. Nat Protoc 11, 1851–1876 (2016). [PubMed: 27606775]
21. Simister NE, Placental transport of immunoglobulin G. Vaccine 21, 3365–3369 (2003). [PubMed: 12850341]
22. Cianga P, Cianga C, Cozma L, Ward ES, Carasevici E, The MHC class I related Fc receptor, FcRn, is expressed in the epithelial cells of the human mammary gland. Hum Immunol 64, 1152–1159 (2003). [PubMed: 14630397]
23. Hurley WL, Theil PK, Perspectives on immunoglobulins in colostrum and milk. Nutrients 3, 442–474 (2011). [PubMed: 22254105]
24. Chen J et al. , Immunoglobulin gene rearrangement in B cell deficient mice generated by targeted deletion of the JH locus. Int Immunol 5, 647–656 (1993). [PubMed: 8347558]
25. Kamada N et al. , Humoral Immunity in the Gut Selectively Targets Phenotypically Virulent Attaching-and-Effacing Bacteria for Intraluminal Elimination. Cell Host Microbe 17, 617–627 (2015). [PubMed: 25936799]
26. Kamada N et al. , Regulated virulence controls the ability of a pathogen to compete with the gut microbiota. Science 336, 1325–1329 (2012). [PubMed: 22582016]
27. Krishnan S, Prasadarao NV, Outer membrane protein A and OprF: versatile roles in Gram-negative bacterial infections. FEBS J 279, 919–931 (2012). [PubMed: 22240162]
28. Seo SU et al. , Intestinal macrophages arising from CCR2(+) monocytes control pathogen infection by activating innate lymphoid cells. Nat Commun 6, 8010 (2015). [PubMed: 26269452]
29. Derrien M, Alvarez AS, de Vos WM, The Gut Microbiota in the First Decade of Life. Trends Microbiol 27, 997–1010 (2019). [PubMed: 31474424]
30. Tamburini S, Shen N, Wu HC, Clemente JC, The microbiome in early life: implications for health outcomes. Nat Med 22, 713–722 (2016). [PubMed: 27387886]
31. Garrett WS et al. , Enterobacteriaceae act in concert with the gut microbiota to induce spontaneous and maternally transmitted colitis. Cell Host Microbe 8, 292–300 (2010). [PubMed: 20833380]
32. van Acker J et al. , Outbreak of necrotizing enterocolitis associated with Enterobacter sakazakii in powdered milk formula. J Clin Microbiol 39, 293–297 (2001). [PubMed: 11136786]
33. Hunter CJ, Upperman JS, Ford HR, Camerini V, Understanding the susceptibility of the premature infant to necrotizing enterocolitis (NEC). Pediatr Res 63, 117–123 (2008). [PubMed: 18091350]

34. Carvalho FA et al. , Transient inability to manage proteobacteria promotes chronic gut inflammation in TLR5-deficient mice. Cell Host Microbe 12, 139–152 (2012). [PubMed: 22863420]

35. McGeachy MJ, Cua DJ, Gaffen SL, The IL-17 Family of Cytokines in Health and Disease. Immunity 50, 892–906 (2019). [PubMed: 30995505]

36. Palm NW et al. , Immunoglobulin A coating identifies colitogenic bacteria in inflammatory bowel disease. Cell 158, 1000–1010 (2014). [PubMed: 25171403]

37. Gopalakrishna KP et al. , Maternal IgA protects against the development of necrotizing enterocolitis in preterm infants. Nat Med 25, 1110–1115 (2019). [PubMed: 31209335]

38. Pabst O, Slack E, IgA and the intestinal microbiota: the importance of being specific. Mucosal Immunol 13, 12–21 (2020). [PubMed: 31740744]

39. Zheng W et al. , Microbiota-targeted maternal antibodies protect neonates from enteric infection. Nature 577, 543–548 (2020). [PubMed: 31915378]

40. Harriman GR et al. , Targeted deletion of the IgA constant region in mice leads to IgA deficiency with alterations in expression of other Ig isotypes. J Immunol 162, 2521–2529 (1999). [PubMed: 10072491]

41. Cascalho M, Ma A, Lee S, Masat L, Wabl M, A quasi-monoclonal mouse. Science 272, 1649–1652 (1996). [PubMed: 8658139]

42. Roh JI et al. , CRISPR-Cas9-mediated generation of obese and diabetic mouse models. Exp Anim 67, 229–237 (2018). [PubMed: 29343656]

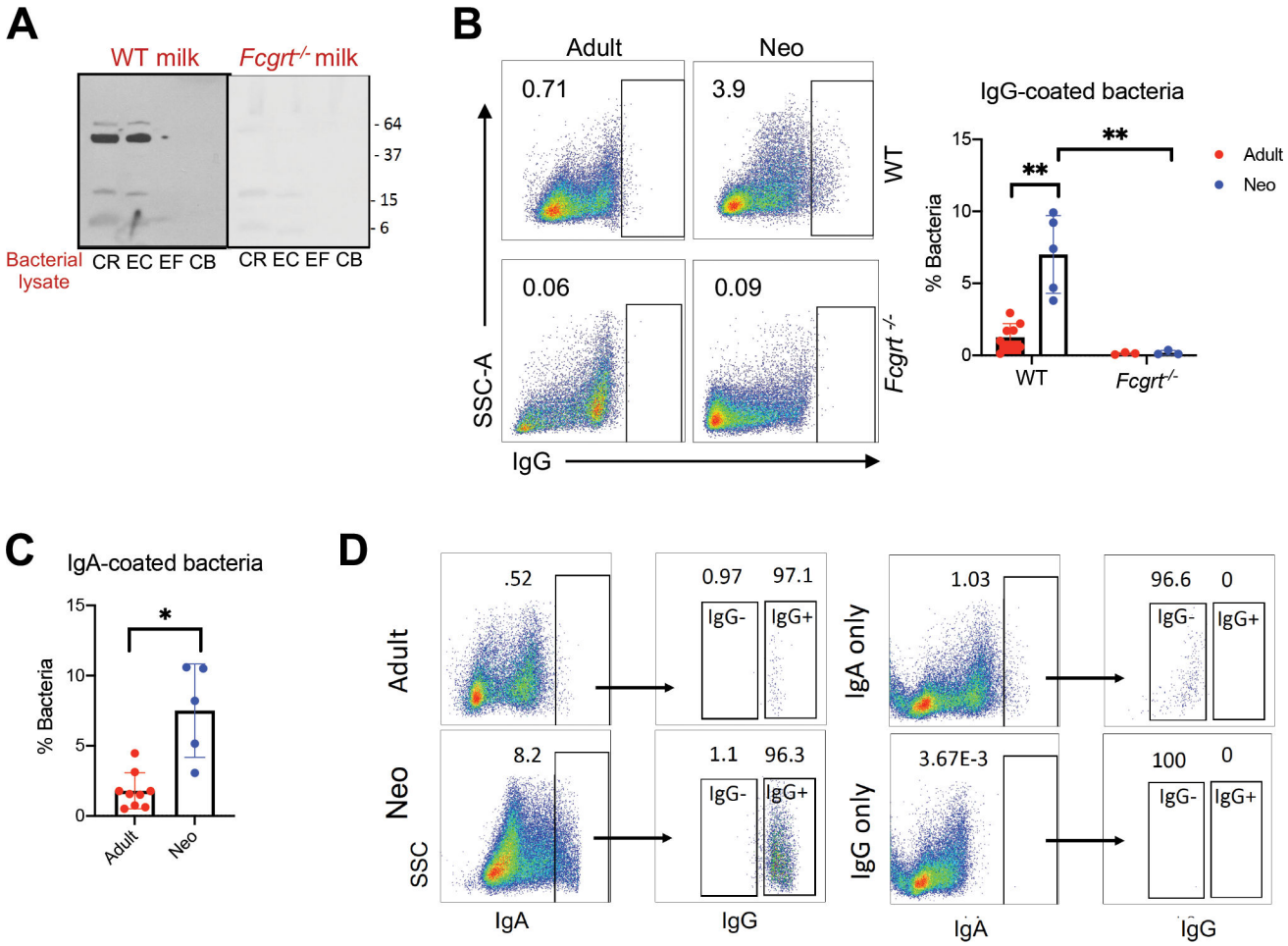

Figure 1. Maternal IgG antibodies are transferred to breast milk through FcRn and coat bacteria in the neonatal intestine.

A. Immunoblotting for mouse milk IgG from naïve WT or *Fcgrt*$^{-/-}$ dams (diluted 1:100) against cell lysates of gram-negative *C. rodentium* (CR), *E. coli* (EC), and gram-positive *Enterococcus faecalis* (EF), *and Clostridium bifermentans* (CB). **B**. Flow cytometry of IgG-coated fecal bacteria from naïve WT or *Fcgrt*$^{-/-}$ adult mice (8–10 weeks old) and neonatal mice (neo; 7 days old). **C**. Flow cytometry of IgA-coated fecal bacteria from naïve WT adult mice (8–10 weeks old) and neonatal mice (7 days old). **D**. Flow cytometry analysis of IgA and IgG coating on fecal bacteria from naïve WT adult mice (8–10 weeks old) and neonatal mice (7 days old). Data are representative of 2 independent experiments. Bar graphs show mean ± SEM with each point representing one mouse. Student's unpaired t-test was used to compare differences between two groups: * $p<0.05$, ** $p<0.01$.

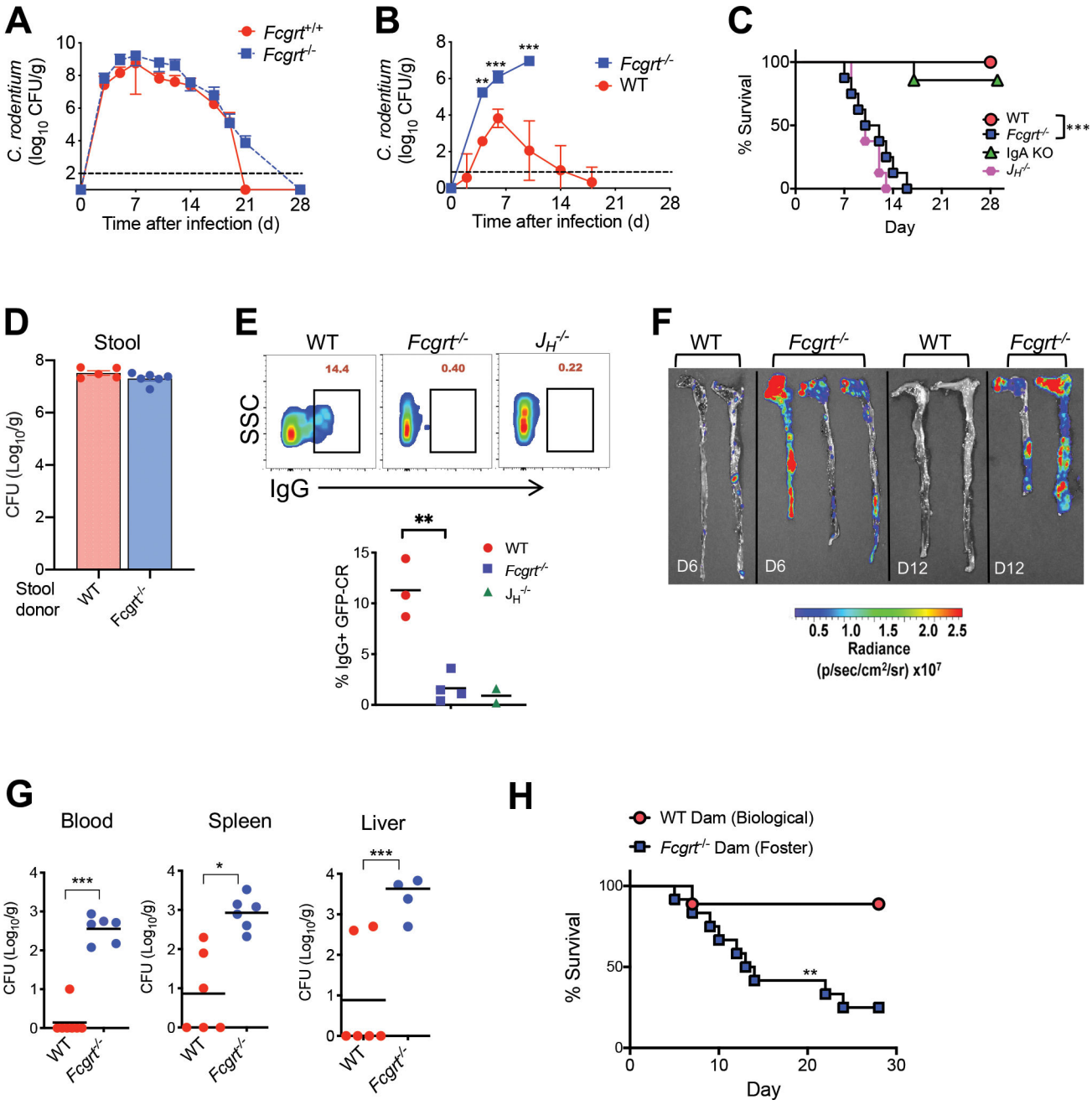

Figure 2. Maternal IgG antibodies inhibit colonization and mucosa-attachment of *C. rodentium* in the neonatal gut.

A. Colony-forming units (CFU) of *C. rodentium* in feces of adult WT and *Fcgrt*$^{-/-}$ mice infected with 10^9 CFU of *C. rodentium* (n=4–6 mice at each time point for each group). **B.** CFU of *C. rodentium* in feces of neonatal WT and *Fcgrt*$^{-/-}$ mice infected with 5×10^7 of *C. rodentium* (n=4–9 mice at each time point for each group). **C**. Survival of WT (n=13), *Fcgrt*$^{-/}$ (n=16), IgA KO (n=10) and B cell-deficient $J_H^{-/-}$ (n=10) neonates (18 days old) after oral infection with 5×10^7 CFU of *C. rodentium*. **D.** CFU of *C. rodentium* in the stool at 3 dpi of P14 GF colonized with fecal bacteria from P14 WT or *Fcgrt*$^{-/-}$ mice for 3 days (n=5–6 mice per group). **E.** IgG-coating of GFP-*C. rodentium* isolated from WT, *Fcgrt*$^{-/-}$

and $J_H^{-/-}$ neonatal mice 6 days after infection. **F**. Imaging of luminescence-expressing *C. rodentium* on the mucosa of the cecum and colon (after removing luminal contents) of WT and *Fcgrt*$^{-/-}$ neonatal mice 6 days or 12 days after infection. **G.** CFU of *C. rodentium* in the blood, spleens and livers of WT and *Fcgrt*$^{-/-}$ mice 6 days after infection. Data represent 2–3 independent experiments. **H**. Survival of WT neonates which were cross-fostered by *Fcgrt*$^{-/-}$ dams (n=12) on day 1 or nursed by biological WT dams (n=9) for 18 days prior to oral infection with 5×10^7 CFU of *C. rodentium*. Data represent two independent experiments. Graphs show mean ± SEM with each point representing one mouse. Student's unpaired t-test was used to compare differences between two groups, and one-way ANOVA with Tukey's multiple comparisons test was used to compare differences between multiple groups: * $p<0.05$, ** $p<0.01$, *** $p<0.005$.

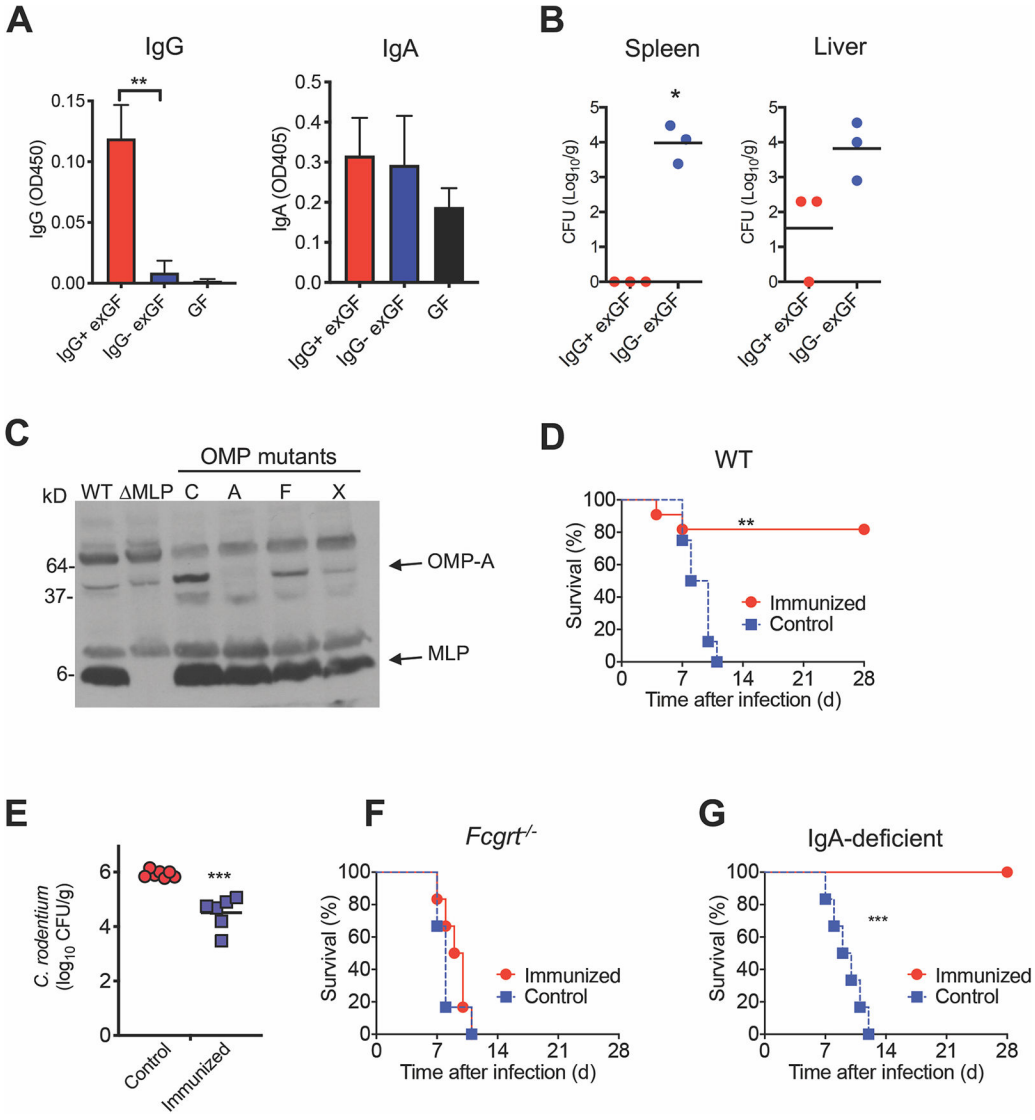

Figure 3. Colonization of IgG-inducing gut bacteria, or maternal immunization with OMP-A, confer protection of neonates against *C. rodentium* via induction of IgG.

A. Induction of fecal bacteria-specific serum IgG and IgA 2 weeks after transplantation of IgG^+ or IgG^- luminal bacteria isolated from 18-day-old WT neonates. **B**. CFU of *C. rodentium* in the spleens or livers of IgG^+ and IgG^- exGF mice after infection with 5×10^7 CFU of *C. rodentium*. **C.** Immunoblotting for IgG antibodies in mouse sera for proteins from lysates of different *E. coli* strains (WT, MLP-deficient, strains deficient in either OMP-C, A, F or X). **D-E**. Survival of WT neonates from dams that had been immunized with OMP-A or without immunization (control) after oral infection with 5×10^8 CFU of *C. rodentium* (**D**) (control: n=11; immunized: n=8), and CFU in the blood of the neonates 6 days after infection (**E**). **F.** Survival of $Fcgrt^{-/-}$ neonates from $Fcgrt^{-/-}$ dams that had been immunized with OMP-A or without immunization (control) after oral infection with 5×10^8 CFU of *C. rodentium* (control: n=6; immunized: n=6). **G**. Survival of IgA-deficient neonates from IgA-deficient dams that had been immunized with OMP-A or without immunization (control) after oral infection with 5×10^8 CFU of *C. rodentium* (control: n=9; immunized:

n=6). Data represent 2–3 independent experiments. Graphs show mean ± SEM with each point representing one mouse. Student's unpaired t-test was used to compare differences between two groups, and one-way ANOVA with Tukey's multiple comparisons test was used to compare differences between multiple groups: * $p<0.05$, ** $p<0.01$, *** $p<0.005$.

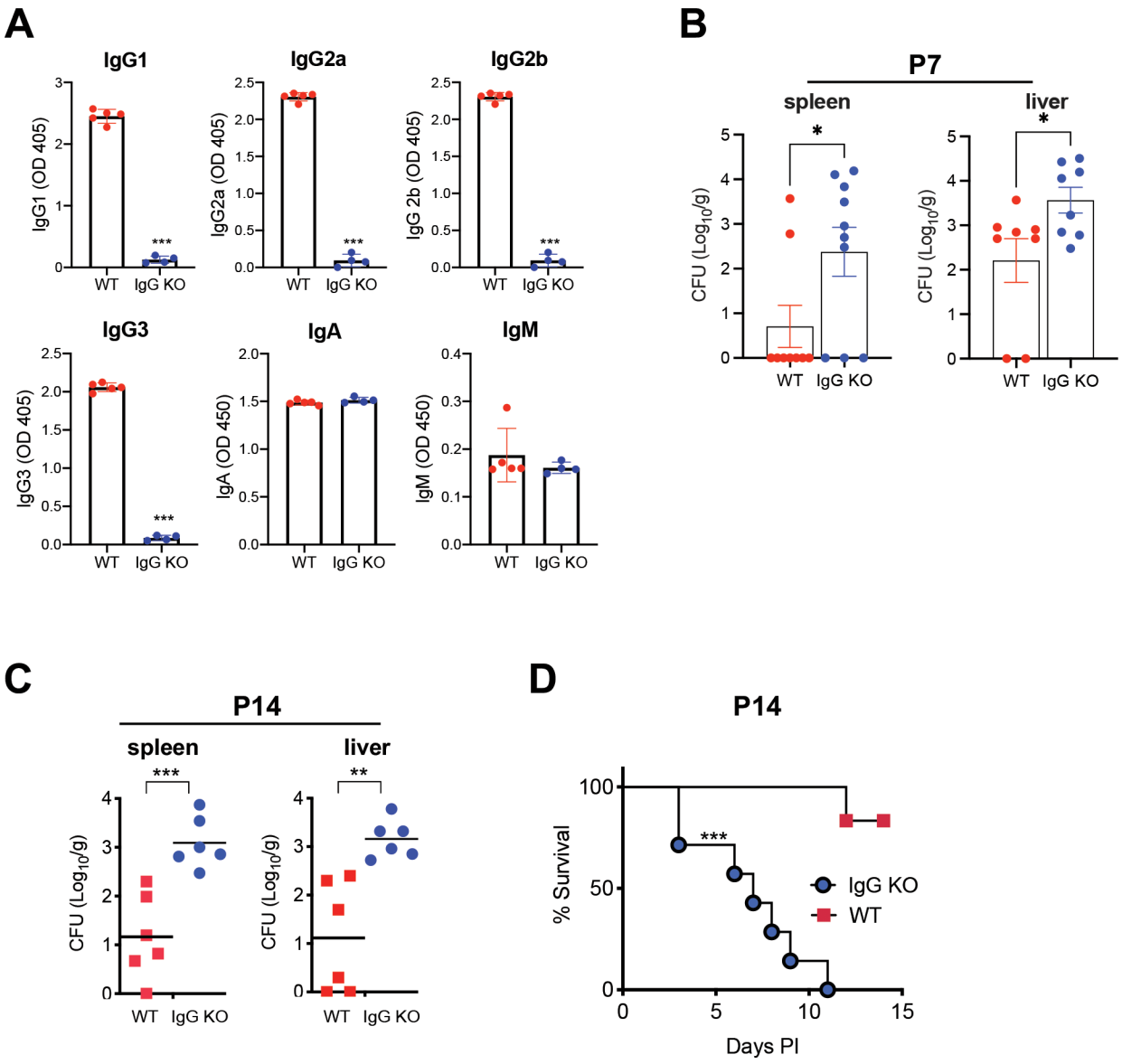

Figure 4. IgG-deficient neonatal mice are more susceptible to enteric *C. rodentium* infection.

A. ELISA measurement of serum IgG1, IgG2a, IgG2b, IgG3, IgA and IgM in adult WT and IgG KO mice (8–10 weeks old). B. CFU of *C. rodentium* in the spleens or livers of day 7 (P7) IgG KO (n=8) and WT (n=8) mice at 3 dpi after infection with 5×10^6 CFU of *C. rodentium.* C-D. CFUs of *C. rodentium* in the spleens or livers of IgG KO (n=6) and WT (n=6) mice at 3 dpi (**C**) and survival (6–7 mice/group) (**D**) after infection with 5×10^7 CFU of *C. rodentium.* Data represent 2–3 independent experiments. Graphs show mean ± SEM with each point representing one mouse. Student's unpaired t-test was used to compare differences between two groups: * $p<0.05$, ** $p<0.01$, *** $p<0.005$.

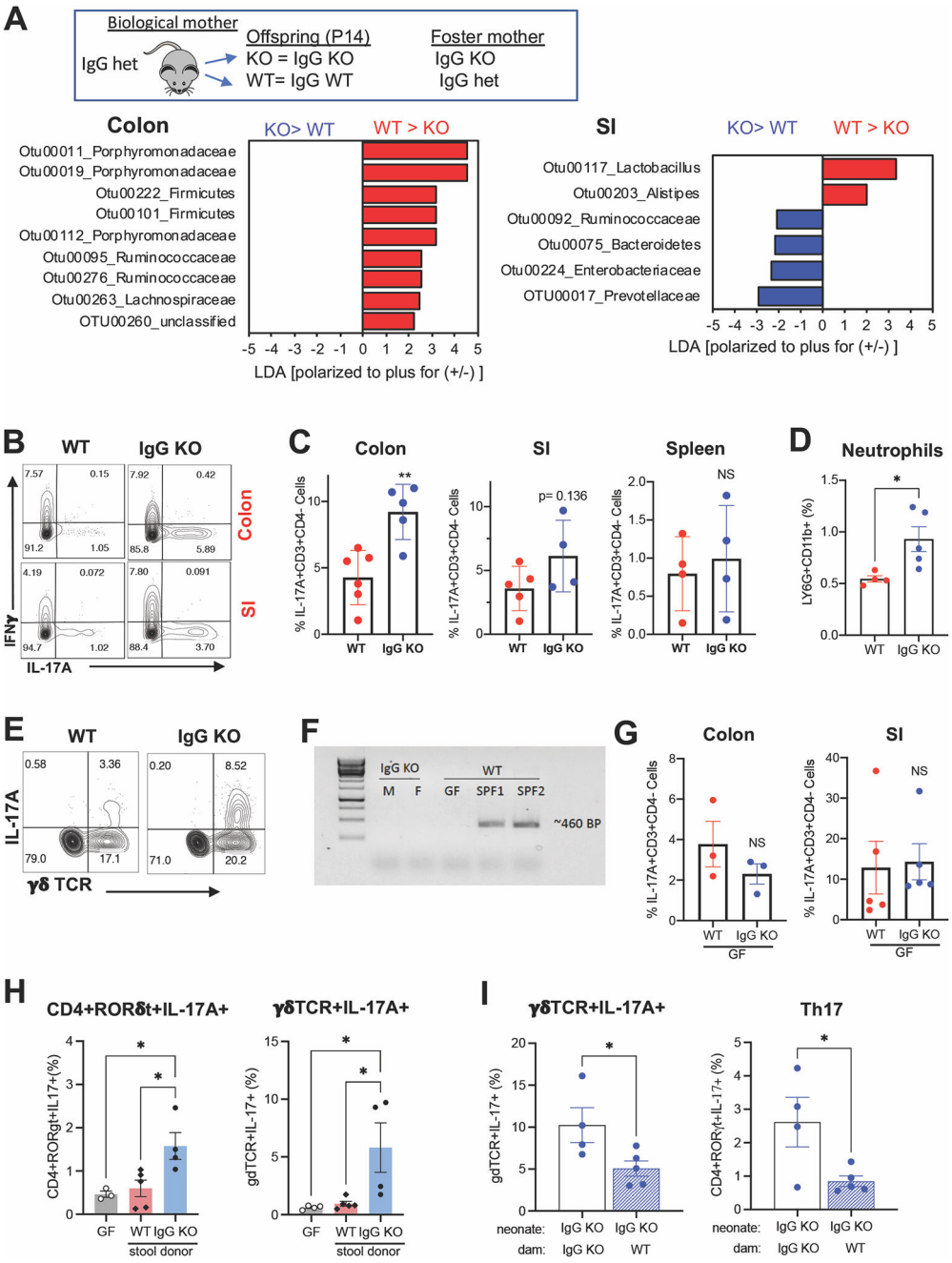

Figure 5. Altered gut microbiota promotes IL-17A$^+$ cells in the intestines of IgG-deficient neonatal mice.

A. LEfSe analysis shows bacterial OTUs in the colon and small intestine that were differentially abundant between IgG KO and littermate WT neonates. 6 neonates of each group were analyzed. **B-E**. Production of IL-17A and IFN**γ** **(B)** within CD3$^+$CD4$^-$CD45$^+$ lamina propria cells isolated from 2-week-old IgG KO and WT neonates. The % of IL-17A-producing cells within CD3$^+$CD4$^-$CD45$^+$ cells in the colons, small intestines and spleens (**C**), and neutrophils in the colons (**D**) were quantified and compared between WT and IgG KO neonates. Colonic IL-17A and γδ TCR expressing cells (**E**). **F**. Rederivation of

IgG KO mice to be germ-free after embryo transfer to a GF foster dam. Fecal DNA from adult offspring (M=male, F=Female) was used for PCR for 16S rRNA (PCR product ~ 460bp) to verify sterility. **G.** The % of IL-17A-producing cells within $CD3^{+}CD4^{-}CD45^{+}$ cells in the colons and small intestines in WT and IgG KO germ-free neonates. **H.** Flow analysis of IL17-producing immune cells in colon lamina propria of GF neonates colonized with fecal bacteria from SPF WT or IgG KO P7 neonates for 2 weeks. **I.** Flow analysis of IL-17A-producing immune cells in the colon lamina propria of P14 IgG KO neonates that were cross-fostered with a WT or IgG KO dam at P1. Data are representative of 2–3 independent experiments. Graphs show mean ± SEM with each point representing one mouse. Student's unpaired t-test was used to compare differences between two groups, and one-way ANOVA with Tukey's multiple comparisons test was used to compare differences between multiple groups: * $p<0.05$, ** $p<0.01$.

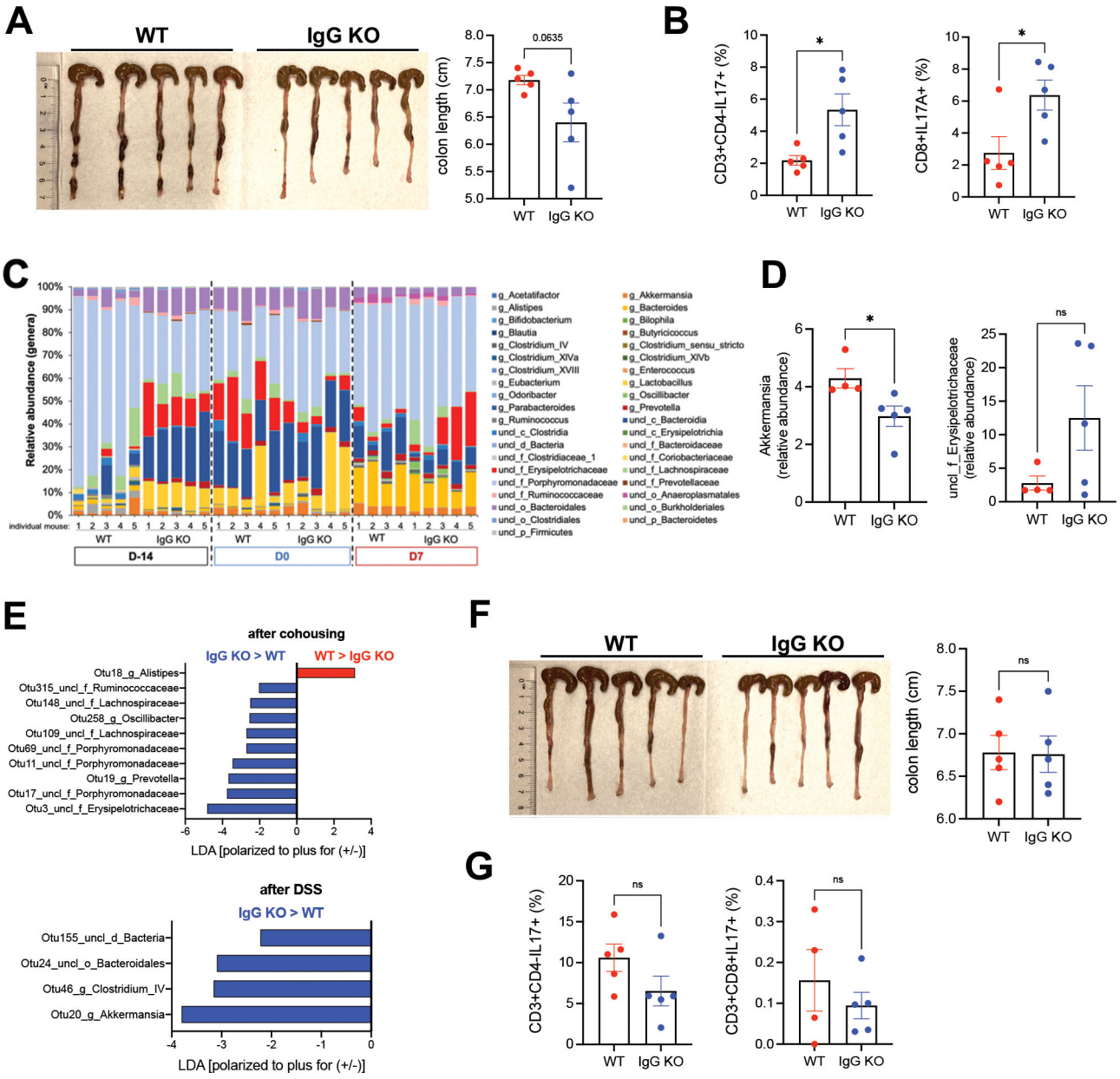

Figure 6. Altered gut microbiome increases susceptibility to DSS-induced colitis in IgG KO adult mice.

A-B. WT and IgG KO adult mice were cohoused for 2 weeks and were then separated prior to treatment with 2% DSS for 7 days. **A.** Representative image of mouse colons and colon lengths after DSS. **B.** Quantification of IL-17A-expressing cells within $CD3^{+}CD4^{-}CD45^{+}$ and $CD3^{+}CD8^{+}CD45^{+}$ lamina propria cells isolated from mouse colons. **C.**16S rRNA sequencing analysis shows relative abundance of bacteria at the genus level in WT vs IgG KO female adult mice colons (age >6 weeks, n=4–5 mice/group) before co-housing (D-14), after co-housing (D0), and after 7 days of DSS in drinking water (D7). Each bar represents a single mouse. **D**) Relative abundance of specific bacteria (genus level) at D7. **E.** LEfSe analysis shows specific bacterial OTUs in the colon that were significantly ($P<0.05$) different between WT and IgG KO adult mice. **F-G.** WT and IgG KO adult mice were

cohoused for 2 weeks prior to DSS treatment and throughout DSS treatment for 7 days. **F.** Representative image of mouse colons and colon lengths after DSS. **G.** Quantification of IL-17A-expressing cells within $CD3^+CD4^-CD45^+$ and $CD3^+CD8^+CD45^+$ lamina propria cells isolated from mouse colons. Data represent 2–3 independent experiments. Graphs show mean ± SEM with each point representing one mouse. Student's unpaired t-test was used to compare differences between two groups: * $p<0.05$.